Bull Earthquake Eng
DOI 10.1007/s10518-017-0177-8

ORIGINAL RESEARCH PAPER

# Advances in rocking core-moment frame analysis

**Mark Grigorian**[1] · **Abdolreza S. Moghadam**[2] · **Hadiseh Mohammadi**[2]

Received: 9 February 2016 / Accepted: 20 June 2017


**Abstract** The paper introduces a number of new analytic techniques and practical technologies that lead to the development of an efficient earthquake resistant system. The proposed structural system consists of a grade beam supported moment frame connected to a rigid rocking core through story level rigid links. The new system tends to bend and tilt as an upright simply supported beam with minimal uniform drift and prevents the formation of soft story failure within the moment frame. It is capable of preventing severe damage to its columns and footings and can be equipped to prevent catastrophic collapse due to strong ground motion and re-center itself afterwards. The analytic development is based on global, design led analysis and results in closed form, exact solutions that are highly suitable for preliminary, manual, as well as spread sheet computations. Several examples have been provided to verify and demonstrate the applications of the proposed formulations. All numerical results have been verified by independent computer analysis.

**Keywords** Earthquakes · Design led analysis · Collapse prevention · Self centering · Damage avoidance · Uniform drift

✉ Abdolreza S. Moghadam
moghadam@iiees.ac.ir

Mark Grigorian
markarjan@aol.com

Hadiseh Mohammadi
H.mohammadi@iiees.ac.ir

[1] MGA Structural. Eng. Inc., 111 N. Jackson St., Glendale, CA 91206, USA

[2] International Institute of Earthquake Engineering and Seismology, Tehran, Iran

Published online: 27 July 2017

## 1 Introduction

Results of decades of research in earthquake engineering have led to the classification of earthquake resisting systems by materials as; *steel, concrete, masonry, wood*, etc., types of system as; *moment frame, bearing wall, building frame, braced frame, cantilever column, dual*, etc., and levels of seismic detailing as; *ordinary, intermediate, special and non-detailed*. Recent studies have resulted in more specific classifications for each material type, e.g., for steel structures as; *ordinary concentric*, *special concentric*, *buckling restrained* and *eccentrically braced frames*, and *special frame/plate shear walls* (FEMA 2009). The vast majority of earthquake resisting structures consist of fixed base Moment Frames (MF) combined with fixed base shear walls and/or braced frames. While these dual systems have served their functions rather well, they are not free from technical flaws and socio-economic drawbacks, yet they remain the most popular construction systems worldwide. To address some of these issues, the authors propose a new dual earthquake resisting system consisting of Grade Beam Supported MFs (GBSMF) in combination with Rigid Rocking Cores (RRC) that promises greater utility and futuristic options than its conventional counterparts.

The idea that rocking motions may reduce damage to structures during earthquakes in not new and was first observed by Housner (1963), half a century ago. The pioneering work in this field is attributed to Aslam et al. (1980), Ajrab (2000), Ajrab et al. (2004), Panian et al. (2007), Deierlein et al. (2009), Seymour and Laflamme (2011), Wada et al. (2012), and Grigorian et al. (2017). The successful use of RCMFs for new and retrofit projects has been reported by Wada et al. (2009, 2012), Janhunen et al. (2012) and Takeuchi et al. (2015). MacRae et al. (2004) and Ji et al. (2009) have proposed similar paradigms in the prevention of large deformations due to drift concentrations in multistory frames.

The theoretical basis of the proposed development together with a number of illustrative examples, have been compiled in Sects. 1–4 of the current article. Sections 5 and 6 discuss the practical design aspects of the proposed solutions. A brief discussion of the proposed structural system is presented in Sect. 7. The loading and configuration of the example problems have been devised to be as general, informative and as tractable as possible. The results of all numerical examples have been verified through independent computer analysis. No specific code issue is discussed. All symbols are defined as they first appear in the text.

### 1.1 Basis for structural system development

While codes of practice do not oppose structural innovations, they recommend design and construction features that are important to seismic performance. These include but are not limited to stable foundations, continuous load paths, adequate stiffness and strength, redundancy, ductility, toughness and ruggedness (ASCE 2007). With these guidelines in mind an attempt is made to propose a viable alternative that is free from the known flaws of fixed base moment frame-structural core combinations. However, instead of dwelling on the flaws of the conventional system, attention is focused on the merits of a proposed system that promises more efficient construction and reliable modes of response than its classical counterparts. The evolution of a new earthquake resisting system or the improvement of an existing one involves the fulfillment of the following developmental steps;

- Definition of system objectives and functional requirements based on sound technical knowledge and observed data. E.g., a system that can sustain the prescribed drift ratio nearly uniformly along its height under all loading conditions, including the *P*-delta effects, with built in provisions for self-centering, reparability, performance control, damage reduction, and collapse prevention. For a simpler example with fewer challenging objectives the interested reader is referred to Grigorian and Grigorian (2015a, b).
- Analytic and or experimental verification of the ability of the system to meet significant performance level objectives. For instance, ASCE 41 (2007) can be referred to for the pertinent acceptability criteria and performance evaluation in the US. Examples of a Moment Frames of Uniform Response (MFUR) that produce target drifts at first yield and incipient collapse can be found in Grigorian and Grigorian (2012).
- Verification of suitability of new components and supplementary devices. The use of such items should be planned and detailed in such a way as not to jeopardize the integrity of other structural members. E.g., standard gap opening and closing beams tend to expand their spans by as much as the gap. Span growth not only induces additional moments on the adjoining columns but also damages column–diaphragm interfaces and results in high drift concentration (Garlock et al. 2007; Dowden and Bruneau 2011). By the same token the interface between a RRC and floor level diaphragms should be carefully detailed and constructed so as not to compromise the integrity of the connection (Grigorian 2015).

The proposed development was greatly inspired by an extensive study of the literature, notably, the well documented synopsis compiled by Hajjar et al. (2013) and the excellent account of rocking frame innovations by Chancellor et al. (2014). The most important lessons learned from these and other sources, for developing a practice friendly earthquake resisting system, can be summarized as follows, that;

- The assumed seismic load distribution should be as close to that generated by the structure as possible.
- The kinematics and boundary conditions of the MF should be selected in such a way as to reduce seismic demand and to prevent damage to columns (especially at supports) and footings.
- The use of a RRC can improve seismic response, prevent soft story failure, and minimize damage to columns, footings and their connections.
- The MF can be connected to the RRC by means of pin ended gap opening Link Beams (LBs) and/or Buckling Restrained Braces (BRBs) at all floor levels.
- The RRC, BRBs and LBs can be used as self-centering and collapse prevention mechanisms. RRCs and LBs can provide firm supports for other supplementary devices (Miller et al. 2011).
- Almost all RCMFs cited in this article have past the tests of experimentation and time-history analysis
- Post-tensioned RRCs and LBs as well as energy dissipating devices, such as BRBs and pressurized fluid dampers retain little to no residual deformations upon removal of the applied load and as such posses inherent collapse prevention and re-centering capabilities (Priestley and Tao 1993). Most importantly some of these devices can be designed to yield at prescribed drift ratios and start energy dissipation at higher rates as required.

These ideas have been combined to develop a new RRC-GBSMF system, also known as rocking wall/core moment frame, (RWMF)/(RCMF) respectively. The practical applications and limitations of these ideas are briefly discussed in the forthcoming section.

## 2 Basic attributes of the proposed dual system

When designed as part of the RCMF, the MF tends to exhibits some of the attributes of structures of uniform shear, such as minimum self weight (Brandt 1978) and uniform demand–capacity ratios close to unity. The more important attributes of RCMF meeting the requirements of the preceding section have been elaborated upon in the following section.

### 2.1 Seismic load distribution

Seismic loading is a function of building mass and stiffness. The conventional triangular distribution suggested by most codes of practice, e.g. ASCE/SEI 7-10, may or may not correspond to the physical realities of a given structure. An approximate or nonconforming seismic distribution can result in unrealistic overturning moments, carrying capacity, elasto-plastic deformations and sequences of formations of plastic hinges. One of the most basic attributes of RRC is that they generate seismic load profiles that are similar to the triangular load distribution. In the proposed structural system, the RRC forces the RCMF to adapt a linear deformation profile and a similar normalized displacement function. While the rigid body rotation of the system changes with monotonic changes in the applied loading, its deformed shape remains the same. The deformed profile is not sensitive to changes in the global stiffness of the MF and its appendages. In fact, the seismic load distribution is a byproduct of the proposed configuration. Furthermore the first natural mode is similar in shape to the displacement profile and suppresses all higher modes of vibrations. The concurrence of the load function and the displacement profiles is significant in that it reduces the differences between the assumed and actual seismic distributions and leads to a number of findings which in turn help formulate a simple but accurate solution to an otherwise complicated problem:

- The dominance of the first mode of vibrations qualifies the system for nonlinear static analysis (FEMA 2005; Deierlien et al. 2010). In other words the results of nonlinear static and dynamic analysis would be in close agreement.
- The similarity of the load and deformation profiles, relates member forces and deformations, the failure load and the mode of collapse to the same normalized straight line. The RRC can sway sideways only. The elastic displacements as well as the plastic hinge patterns of the failure mechanism remain compatible with the tilted profile of the wall (FEMA 2005; Deierlien et al. 2010).
- The force–displacement relationship of the RCMF can be expressed as the function of a single variable for all loading conditions. In other words the elasto-plastic drift ratio can always be expressed in terms of the overturning moment and the effective global stiffness of the system.
- The uniformity of the drift function allows the structure to be treated as a SDOF system or as the assembly of similar subframes stacked on top of each other. Since the drift ratio is the same for all subframes then the demand–capacity ratios of all such

subframes would also be the same. This makes the structure ideally suited to equal energy treatment for base shear computations.

- The structure can be designed as a MF of Uniform Shear (MFUS). Uniform drift can be associated with uniform demand–capacity–stiffness ratios. Therefore almost all structural elements can be selected in accordance with rules of uniform shears or uniform sections. A description of MFUS is presented in Sect. 6.2 below.
- The system lends itself well to Quasi-determinate, design led manual analysis. i.e., groups of similar elements such as beams, columns, braces, links and their connections can be studied as independent groups of members.
- The normalized displacement function is a straight line and remains unchanged throughout the loading history of the system. Loss of stiffness changes the value of the drift angle but not the drift profile. This means that the effective period of the structure can be expressed as a function of the design drift ratio, $\phi_d$ at the centre of mass of the structure, $h_e$ i.e. $T_{eff.} = 2\pi\sqrt{\phi_d h_e/g}$.
- Uniform drift or zero drift concentration reduces the *P*-delta effects and residual displacements (MacRae and Kawashima 1997). *P*-delta moments tend to accelerate collapse. In case of RCMFs, P-delta moments are much more evenly distributed than for the corresponding free standing MFs.

## 2.2 Frame boundary support conditions

Some of the technical advantages of GBSMF as depicted in Fig. 1a, over fixed base frames can be summarized as follows;

- The drift ratios of well proportioned GBSMF at incipient collapse are smaller than those of identical frames with fixed and pinned boundary conditions (Grigorian and Grigorian 2013). For fixed base MFs the abrupt change of stiffness from base to first level produces a sharp concentration of the drift ratio and increases the corresponding angle of rotation.
- Being more flexible, GBSMF tend to attract smaller seismic forces than their fixed base counterparts. The global rotational stiffness of GBSMF is always smaller than those of the geometrically similar fixed base systems.
- GBSMF attract substantially less residual stresses and deformations due to strong ground motion. The stiffnesses of the grade beams are selected in such a way as not to cause drift concentration at the base.

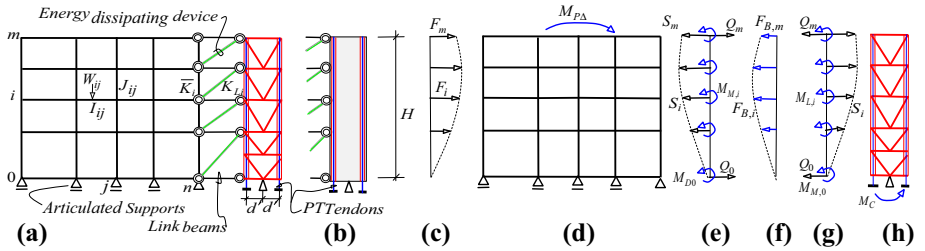


**Fig. 1** **a** GBSMF with braced RRC and supplementary devices, **b** concrete RRC, **c** lateral loading, **d** free standing GBSMF, **e** interactive forces and gap opening moments acting on the frame, **f** assumed BRB reactions, **g** interactive forces and gap opening moments acting on the RRC, **h** braced RRC and base restoring moment

- In GBSMF overturning moments are transmitted to the footings through axial reactions only. Stated differently, no moments are transmitted to the footings. No anchor bolt, base plate and footing damage can occur due to seismic moments.
- The grade beams prevent the formation of plastic hinges at column supports and provide means of controlling column base rotation and the overall drift. The premature formation of plastic hinges at the column supports of fixed base frames is tantamount to releasing the rotational restraints of the supports. The strong column–weak beam condition is implemented at both ends of grade beams.
- Uniform drift or tilt causes all points of contraflexure to move towards mid spans. This implies equal end moments for all frame members and minimal drift for the entire system.

## 2.3 Attributes of rigid rocking core

The physical behavior of RCMF can best be visualized by the frame restraining the RRC in place, and the core imposing uniform or near uniform drift along the height of the frame, Figs. 1a and 2g. However, some of the more relevant, but not less significant attributes of the RRCs can be summarized as follows;

- The high rigidity of the wall causes all wall attached supplementary devices to absorb proportional amounts of energy.
- The RRC tends to rotate as a rigid body without significant in-plane deformations. If needed, a post tensioned core can be activated to prevent collapse and initiate self centering. It can also provide supports for story level auxiliary devices such as LBs, the BRBs etc.
- The RRC helps reduce axial forces in the frame. This increases moment capacities and reduces costs. A large proportion of axial forces due to overturning moments are absorbed by the RRC.
- The RRC tends to redistribute seismic moments very evenly between groups of similar member such as beams and columns of equal spans and heights respectively. In MFUS the core absorbs the entire seismic force and exerts a self balancing reaction on top of the frame that creates a constant racking shear along the height of the frame. Member moments are in direct proportion with racking moments.
- The RRC can enforce the desired mode of failure, but can not increase the carrying capacity of the free standing structure. The RRC is an unstable mechanism, and as such can not influence the kinematics of any other mechanism.
- The RRC tends to bend as an upright simply supported beam rather than a vertical cantilever. The base pivot provides two degrees of restraints. The MF adds one more

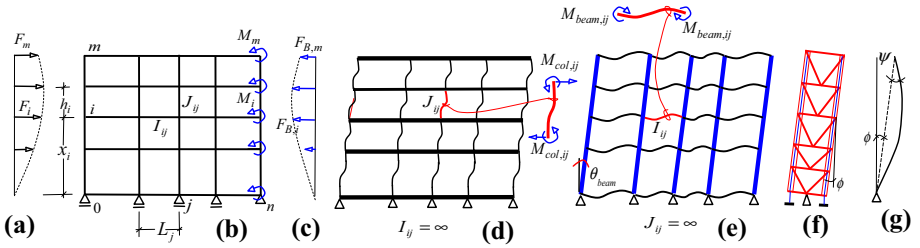


**Fig. 2** **a** Lateral loading, **b** free standing GBSMF with gap opening moments, **c** reactions due to BRBs, **d** GBSMF with rigid beams, **e** GBSMF with rigid columns, **f** tilted RRC, **g** deformation of the combined structure

lateral restraint and makes the core act as a statically determinate beam. Therefore, it may be assumed that the reference line of displacements passes through both the pin and the free end of the core.

- RRCs need not be overwhelmingly rigid. However they should be stiff and strong enough to enforce an almost uniform drift and prevent soft story failure. The ultimate strength of the RRC should be greater than that of the MF and the supplementary devices. The stiffness of the RRC should be selected in such a way as to reduce its own maximum drift to less than a fraction of the prescribed design drift ratio.
- Vertically post-tensioned rigid cores such as concrete or steel shear walls and braced frames can be designed to remain entirely elastic after frame failure. The lateral restoring capabilities of the energized RRC mechanism are defined by its ultimate strength and rotational stiffness respectively. Instead of using axial springs at the ends of the RRC, an equivalent rotational scheme has been utilized to capture the restraining effects of the post tensioned cables.

### 2.4 Attributes of rigid link beams

The function of the LB as a tensioned rocking moment connection is to transfer diaphragm shear, add stiffness to the structure, dissipate seismic energy through gap opening, and provide leverage for self-centering and collapse prevention, Fig. 1a. Usually it consists of prismatic reinforced concrete or steel beams with flat bearing surfaces at both ends. The conventional LB systems, with few exceptions (Garlock et al. 2007), tend to expand their spans beyond the original length. As the gap widens, the beams rotate rigidly and bend the column in proportion to the gap. This in turn reduces the effective post tensioning force and severely damages the beam–column–diaphragm interfaces. The use of fully flat end LBs is not encouraged instead a number of modified link beam systems are suggested Fig. 7a, c. The proposed link beams consist of full length, relatively rigid, axially strong elements with provisions for post tensioning cables. Some of more important issues associated with the use of such LBs are listed below.

- The ends of the proposed link beam may be beveled as proposed by Dowden and Bruneau (2011) or truncated (2015), as in Fig. 7a, c, to avoid full contact between the ends of link and the adjoining members. In order to reduce full contact between the supports and the truncated ends, the width of the minimum cut back should be larger than the expected gap.
- The LB is activated in response to the target drift angle $\phi$ due to external forces $F$. Gap opening or decompression generates an internal couple or moment of resistance $Tl_a$, where $T$ is the total tendon force and $l_a = d/2$ is the lever arm between the line of action of $T$ and the centre of compression. The effects of these moments should be reflected in the design of the MF as well as the RRC.
- Gap opening and closing need not necessarily occur between contact surfaces. It can take place between any two adjacent planes at right angles to the axis of the beam. Gap opening is accompanied with changes in the initial stresses of the post tensioned tendons.
- The response of the LB is sensitive to its layout, the pre-stressing force and the offset distances from the center lines of the adjoining columns $D_{left}$ and $D_{right}$. The effect of such offsets is to increase the gap angle from $\phi$ to $\bar{\phi} = \phi[l + D_{left} + D_{right}]/l = \alpha\phi$. $l$ is the length of the LB. The special cable layouts of Fig. 7 are meant to eliminate loss of stretch due to simultaneous gap opening and closing at opposite ends of the same LB.

- The gap opening and closing property of the LB can best be symbolized by equivalent rotational elastic springs at each end. The equivalent rotational stiffnesses of the post tensioned LBs at the wall and frame side are given as $K_L$ and $K'_F$ respectively.
- Gap movements at the ends of the Ladd natural damping and provide opportunities for self centering, damage reduction and collapse prevention. Such devices reduce frame moments and drift ratios.

### 2.5 Supplementary devices

Several generic and commercially available supplementary damping devices with variable degrees of efficiencies have been used as parts of RCMF systems. BRBs (Taylor devices), Slotted–bolted-friction connections (Grigorian et al. 1995) and post-tensioned gap opening systems (Panian et al. 2007) appear to have been utilized more frequently than others. In this paper BRBs and stressed tendons have been used primarily as means of collapse prevention and self centering rather than damping elements.

## 3 The theoretical approach

The major components of a typical RCMF consisting of the MF, the RRC, the LB and BRB are shown in Fig. 1a. Fortunately, this seemingly complicated structure lends itself well to a very simple analytic solution. The challenge is to untangle the interactive performances of the major components of the system. This is achieved by looking at the problem from a global rather than elemental point of view and resorting to design led analysis and treating the responses of groups of similar elements, such as beams columns, braces, etc., as the constitutive components of the structure. In design led analysis the drift ratio, stability and failure conditions are imposed rather than investigated. The conceptual design of RCMFs with a view to collapse prevention and self centering involves in depth understanding of the physical phenomena surrounding the following issues;

- The relationship between the global rotational stiffness $K^*$ and any expected drift ratio $\phi$.
- The relationship between the global rotational stiffnesses $K_F$ and $K'_F$ of the MF, $K_L$ of the LB, $K_B$ of the BRBs and $K_C$ of the RRC, needed to sustain the drift ratio $\phi$.
- The relationship between the rotational stiffnesses $K'_F$ of the MF, as influenced by the LB moments, needed to oppose $\phi$ by as much as $\varphi$.
- The magnitude of the effective overturning moment, $\mathrm{M}_{eff.}$ acting on the structure? and
- The ultimate lateral capacity of the system.

Knowing that the entire structure tends to respond as a single degree of freedom system, the answer to the first three issues may be found in the simple linear relationships;

$$\phi = \frac{\mathrm{M}_{eff.}}{K^*}, \quad \phi_F = \frac{M_F}{K_F}, \quad \varphi_F = \frac{M_L}{K'_F}, \quad \phi_L = \frac{M_L}{K_L}, \quad \phi_B = \frac{M_B}{K_B} \quad \text{and} \quad \phi_C = \frac{M_C}{K_C} \tag{1}$$

Subscripts ***F, L, B*** and ***C*** refer to MF, LB, BRB and the RRC respectively. The answer to the third concern is that the total external overturning moment $M_0$ is magnified or accompanied with the global *P*-delta moment, $M_{P\Delta}$ which leads to the effective overturning moment $\mathrm{M}_{eff.} = M_0 + M_{P\Delta}$. The intuitive answer to the last question may be expressed as;

$$\mathrm{M} = M_0 + M_{P\Delta} - (M_B + 2M_M + M_C) \tag{2}$$

Here M describes the total moment of resistance of the beams of the frame. A poof of statement (2) is presented in Sect. 3 below. The elegance and power of Eq. (1) is in that it allows the external effects as well as the contributions of all resisting elements and supplementary devices to be expressed as global moments. For instance the net effect of the lateral forces of Fig. 1c can be replaced with their equivalent overturning moment $M_0$. Conversely, the effect of any global moment can be simulated by equivalent horizontal force acting at roof level.

### 3.1 Global elastic response of the frame

Consider the lateral displacements of the GBSMF of Fig. 1a, under gravity loads $W_{i,j}$, lateral loading $F_i$, Fig. 1c, opposing brace forces $F_{B,i}$, Fig. 1f, gap opening moments $M_i$ of Fig. 1e and rigid core restoring moments $M_C$ of Fig. 1h. Figure 1e, g depict the distribution of the interactive forces between the frame and the RRC. The influence of gravity loads $W_{i,j}$ on the lateral displacements of the MF has been studied in some detail in Sect. 4 below. The intricate conditions associated with the use of rigid LBs and BRBs as parts of the RCMF require the load–displacement relationship of each case to be studied separately. The rigid core imposes a uniform drift ratio $\phi$ on the entire structure. The drift ratios of each supplementary device can be studied in terms of the corresponding beam and column rotations, i.e.

$$\phi_F = \theta_{col,F} + \theta_{beam,F}, \quad \phi_M = \theta_{col,M} + \theta_{beam,M} \quad \phi_B = \theta_{beam,B} + \theta_{col,B} + \varphi \quad \text{and} \quad \phi_C = \phi \tag{3}$$

$\theta_{col.}$ and $\theta_{beam}$ stand for rotations due to column and beam bending respectively. Since the sum of all end moments due to external moments $M_i$ is zero then $\theta_{col,M} = 0$. Next, assuming that the secondary effects due to brace movement are negligible, then $\theta_{beam,B} = \theta_{col,B} = 0$. Hence, the frame rotation may be equated to the rigid body tilt $\varphi$, of the system, in which case Eq. (3) can be simplified as; $\phi_F = \theta_{col,F} + \theta_{beam,F}$, $\phi_M = \theta_{beam,M}$,$\phi_B = \varphi$ and $\phi_C = \phi$. The net lateral story level displacements of the combined structure, Fig. 2a, can be computed as;

$$\Delta_i = (\phi_F - \phi_M - \phi_B - \phi_C)x_i = \phi x_i \tag{4}$$

### 3.2 Free standing frame under lateral forces $F_i$

Since $\phi$ is constant it would be convenient to compute $\theta_{col.}$ and $\theta_{beam}$ independently, assuming the other is zero. Figure 2d, e depict the imaginary scenarios where $\theta_{beam} = 0$ or $I_{i,j} = \infty$ and $0 > J_{i,j} > \infty$, and $\theta_{col.} = 0$ or $J_{i,j} = \infty$ and $0 > I_{i,j} > \infty$ respectively. If the resulting end moments of column $i$, $j$ due to the former condition is denoted by $M_{col.ij} = 6E\bar{k}_{ij}\theta_{col.F}$, where $\bar{k}_{ij} = J_{ij}/h_i$, then the sum of all column moments should balance the total external overturning moment;

$$M_0 + M_{P\Delta} = 2\sum_{j=0}^{n}\sum_{i=1}^{m} M_{col,ij} = 12E\theta_{col.F}\sum_{j=0}^{n}\sum_{i=1}^{m}\bar{k}_{ij} \tag{5}$$

A simple method of computing the global $P$-delta moment is presented in Sect. 3.7 below. Similarly, if the resulting end moments of beam $i$, $j$ due to the latter condition are

given by $M_{beam.ij} = 6Ek_{ij}\theta_{beam.F}$, where $k_{ij} = I_{ij}/L_j$, then the sum of all internal beam moments should also balance the total external overturning moment;

$$M_0 + M_{P\Delta} = 2\sum_{j=0}^{n}\sum_{i=1}^{m} M_{beam,ij} = 12E\theta_{beam.F}\sum_{j=1}^{n}\sum_{i=1}^{m} k_{ij} \tag{6}$$

Substitution of Eqs. (5) and (6) into $\phi_F = \theta_{col,F} + \theta_{beam,F}$, gives;

$$\phi_F = \theta_{col,F} + \theta_{beam,F} = \frac{(M_0 + M_{P\Delta})}{12E}\left[\frac{1}{\sum_{j=0}^{n}\sum_{i=1}^{m}\bar{k}_{i,j}} + \frac{1}{\sum_{j=1}^{n}\sum_{i=0}^{m}k_{i,j}}\right] = \frac{(M_0 + M_{P\Delta})}{K_F} \tag{7}$$

Equations (1) and (7) are ideally suited for estimating the rotational stiffness of the subject moment frame. Examples 1 and 2 below have been devised to verify the accuracy and usefulness of Eq. (7). Example 1 describes the response of a 9 story MF as part of a RCFM, where the RRC imposes a uniform drift ratio $\phi$ upon the MF. Example 2 deals with the response of an un-supplemented 10 story free standing MF, with similar external dimensions, global rotational stiffness and lateral loading designed to sustain the same uniform drift $\phi$ as for Example 1.

*Example 1* GBSMF + RRC.

Consider the static response of the steel MF of a $m \times n\,(9 \times 10)$ RCMF, under a roof level lateral force $F = 100$ kips with no supplementary devices, designed to sustain a uniform drift ratio $\phi$ along its height. Compute $\phi$ and $\Delta_m$ provided that; $h_1 = h_2 = 15$ ft, $h_3 = h_4 = h_5 = h_6 = h_7 = h_8 = h_9 = 10$ ft, $L_j = L = 2h$, E = 29,000 ksi. Assume $M_{P\Delta} = 0$. $J_{1,0} = J_{1,10} = J_{2,1} = J_{2,10} = 448$ in$^3$ (W16 × 36), $J_{1,1} - J_{1,9} = J_{2,1} - J_{2,9} = 890$ in$^3$ (W18 × 55), $J_{3,0} - J_{3,9} = J_{3,10} = J_{9,10} = 199$ in$^3$ (W14 × 22), all other $J_{i,j} = 391in^3$ (W12 × 50), $I_{0,j} = I_{9,j} = 118$ in$^3$ (W10 × 22), $I_{1,j} = I_{2,j} = 350$ in$^3$ (W12 × 45), all other $I_{i,j} = 238$ in$^3$ (W12 × 30).

**Solution** $M_0 = 100 \times 100 = 10{,}000$ kip ft,

$$\sum_{j=0}^{n}\sum_{i=1}^{m}\bar{k}_{i,j} = (2 \times 199 + 9 \times 391)7/h + (2 \times 448 + 9 \times 890)2/1.5h = 39{,}294/h$$

$$\sum_{i=0}^{m}\sum_{j=1}^{n}k_{i,j} = (2 \times 118 + 6 \times 238)10/L + (2 \times 350)10/L = 23{,}640/L$$

From Eq. (7); $\phi = \frac{10{,}000 \times 12^2}{12 \times 29{,}000}\left[\frac{10}{39{,}294} + \frac{20}{23{,}640}\right] = 0.004554$ (0.004542), consequently;

$\Delta_{10} = 0.004554 \times 1200 = 5.4648$ in. (5.4440 in). Numbers in parenthesis correspond to computer analysis.

*Example 2* Free standing GBSMF with no supplementary devices.

Consider the static response of a $m \times n\,(10 \times 10)$ free standing, regular GBSMF under a roof level lateral force $F = 100$ kips, designed to sustain a uniform drift ratio $\phi$ along its height. Compute $\phi$ and $\Delta_m$ provided that;

$h_i = h = 10$ ft, $L_j = L = 2h$, $J_{1,i} = J_{10,i} = 199$ in$^3$ (W14 × 22). All other $J_{i,j} = 391$ in$^3$ (W12 × 50). $I_{0,j} = I_{m,j} = 118$ in$^3$ (W10 × 22), all other $I_{i,j} = 238$ in$^3$ (W12 × 30). Assume $M_{P\Delta} = 0$.

**Solution** $M_0 = 100 \times 100 = 10{,}000$ kip ft,

$$\sum_{j=0}^{n}\sum_{i=1}^{m}\bar{k}_{i,j} = (2 \times 199 + 9 \times 391)10 = 39{,}170/h \quad \text{and}$$

$$\sum_{i=0}^{m}\sum_{j=1}^{n}k_{i,j} = (2 \times 118 + 9 \times 238)10 = 23{,}780/L$$

From Eq. (6) $\phi = \frac{10{,}000 \times 12^2}{12 \times 29{,}000}\left[\frac{10}{39{,}170} + \frac{20}{23{,}780}\right] = 0.004536$, $K_F = 2{,}204{,}342.55$ kip ft/radians and

$$\Delta_{10} = 0.004546 \times 1200 = 5.4438 \text{ in. } (5.4440 \text{ in}).$$

It may be seen that the results of the two examples coincide. The first important conclusion drawn at this stage is that Eq. (7) is powerful enough to predict the drift ratios of any RCMF as well as MFUR. The MFUR are a class of un-supplemented free standing MF that is capable of sustaining straight line lateral displacement profiles under lateral loading. In MFUR the ratio of subframe (*racking moment/rotational stiffness*) is constant along the height of the structure otherwise the system can not be qualified as an MFUR. The second more important, but less obvious finding is that if the RCMF and MFUR can produce the same lateral displacement under the same loading conditions then their combination may be regarded as counterproductive. Comparing Examples 1 and 2, it may be seen that the moment frame of Example 2 is not suitable for RCMF applications. The subject is further elaborated upon in Sect. 6 below. However since the MF of Example 2 offers a more tractable configuration it will be used as the reference model of all other examples presented in the forthcoming sections of this article.

### 3.3 Frame reacted by link beams (under end moments $M_M = M_L$)

Let $M_i$ represent the opposing moments generated at the ends of the link beams. Following the rationale presented in Sect. 3.2, the effects of $M_i$ on the moment frame can be expressed as;

$$\varphi_F = \theta_{beam,F} = \frac{\sum_{i=0}^{m} M_i}{12E\sum_{j=1}^{n}\sum_{i=1}^{m}k_{i,j}} = \frac{M_M}{K'_L} \tag{8}$$

$M_M$ is the total moment of resistance generated by the frame side end of all link beams, and as such may be treated as a restoring moment. It can also be related to the gap opening angle $\bar{\phi}$ and the LB rotational stiffness $k_{L,i}$. i.e.

$$M_M = M_L = \sum_{i=0}^{m} M_i = \sum_{i=0}^{m} k_{L,i}\bar{\phi} = \bar{\phi}\sum_{i=0}^{m} k_{L,i} = \alpha\phi K_L \tag{9}$$

The relationship between the tendon force $T_{ten}$, angle $\bar{\phi}$ and the corresponding tendon extension may be expressed as; $\bar{\phi} = \alpha\phi = \frac{2T_{ten}L_{ten}}{dA_{ten}E} = \frac{4T_{ten}dL_{ten}}{2d^2A_{ten}E} = \frac{M_i}{k_{L,i}}$ and $k_{L,i} = \frac{d^2A_{ten}E}{4L_{ten}}$. It is

instructive to study the interactive effects of the MF and the LBs at this stage. Total moments $M_M = M_L$ at the two ends of all LBs tend to reduce the drift ratio by bending the MF and tilting the RRC in opposite direction to the applied loading, thus;

$$\phi = \frac{(M_0 + M_{P\Delta} - M_M)}{K_F} - \frac{M_M}{K'_F} = \frac{(M_0 + M_{P\Delta} - K_L\phi)}{K_F} - \frac{K_L\phi}{K'_F} \quad \text{or} \quad \phi_F = \frac{(M_0 + M_{P\Delta})}{[1 + \bar{K}]K_F} \tag{10}$$

where $\bar{K} = K_L[(1/K'_F) + (1/K_F)]$ and $K_F(1 + \bar{K})$ may be regarded as the percentage contribution of the LBs and the equivalent rotational stiffness of the MF respectively. This finding is particularly useful for retrofit projects. If for any reason $\phi_F$ exceeds $\phi_{Rqd.}$ or $K_F$ is deemed inadequate then Eq. (10) may be utilized to asses the additional stiffnesses needed to satisfy the issue, thus;

$$K_L = \left[\frac{(M_0 + M_{P\Delta})}{K_F\phi_{rqd.}} - 1\right]\frac{K'_F K_F}{K'_F + K_F} \tag{11}$$

It is also instructive to note that as plastic hinges form at the ends of the beams of the frame, the relative stiffness ($k_{i,j} = EI_{i,j}/L_j$) of all beams become zero. In theoretical terms, while the rotational springs hold the frame together, $k_{i,j}$ tend toward zero and Eq. (10) reduces to; $\phi_F = (M_0 + M_{P\Delta})/2K_L$. This can be attributed to the ability of the proposed LB arrangement which can supply a total restoring moment of $2M_i$ to the combined structure.

*Example 3* Determination of LB stiffness.

Following Example 2 and assuming that the BRBs and the RRC are not active, i.e., $K_B = K_C = 0$, compute the additional stiffness of each LB needed to lower the drift ratio to $\phi = 0.003$ radians provided that;

$$k_{L,i=0} = k_{L,i=m} = k_L/2 \quad \text{and} \quad k_{L,i=1\ldots m-1} = k_L, \quad \text{i.e.} \quad K_L = mk_L.$$

**Solution** From Eq. (8) $K'_L = 12 \times 29{,}000 \times 23{,}780/20 \times 12^2 = 2{,}873{,}416.67$ kip-ft/radians, and Eq. (11) gives; $K_L = \left[\frac{10{,}000}{2{,}204{,}342.55 \times 0.003} - 1\right]\left[\frac{2{,}204{,}342.55 \times 2{,}873{,}416.67}{2{,}204{,}342.55 + 2{,}873{,}416.67}\right] = 1{,}247{,}399.55$ kip-ft/radians. Let, $k_M = K_L/m$, then; $k_M = 124{,}739.96$ kip-ft/radians, $M_i = \phi k_M = 0.003 \times 1{,}247{,}399.55 = 187.12$ kip-ft. This implies that $M_0 = M_{10} = 93.56$ kip-ft and $M_i = 187.12$ kip-ft, $i = 1, 2\ldots9$, acting along the end column at $n = 10$. From Eq. (8); $M_M = mM_i = 1871.24$, hence $\phi_M = \frac{2 \times 1871.24}{1{,}247{,}399.55} = 0.003(0.003)$ radians, and $\Delta_{10} = 0.003 \times 1200 = 3.60$ in. (3.55 in). Once again computer analysis confirms the results.

### 3.4 Frame supplemented with diagonal braces (resistive moments $M_B$)

The purpose of this section is to assess the contribution of the diagonal BRBs of Fig. 3c to the global stiffness of the structure. This is achieved by assuming that all members of the imaginary braced frame, including the common vertical with the MF are infinitely rigid and constitute an unstable mechanism as shown in Fig. 3b. All diagonals are pin ended axially hysteretic BRBs. This is a conservative assumption and slightly underestimates the drift reduction capacity of the imaginary braced system. Following Eq. (37), the axial

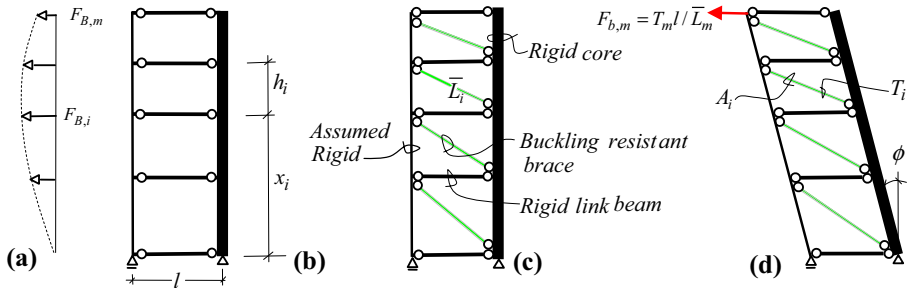


**Fig. 3** **a** Equivalent notional lateral load corresponding to $T_i$, **b** imaginary rocking mechanism, **c** braced frame with BRB, **d** rigid body rocking of the braced frame and roof level reaction

deformations $\bar{\Delta}_i$ of any such brace can be related to the uniform drift ratio, i.e. $\bar{\Delta}_i = \frac{\alpha\phi h_i l}{L_i} = \frac{T_i \bar{L}_i}{A_i E_{brc}}$, $T_i = \frac{\alpha\phi h_i l A_i E_{brc}}{\bar{L}_i^2}$ or $A_i = \frac{T_i \bar{L}_i^2}{\alpha\phi h_i l E_{brc}}$. Considering the rigid body rotation $\phi_B$ of Fig. 3d, the virtual work concept leads to;

$$\sum_{i=1}^{m} F_{B,i}\phi x_i = \phi M_B = \sum_{i=1}^{m} T_i \bar{\Delta}_i = \sum_{i=1}^{m} \left[\frac{\alpha^2\phi^2 h_i^2 l^2 A_i E_{brc}}{\bar{L}_i^3}\right] \quad \text{or}$$
$$\phi_B = \frac{M_B}{\alpha^2 l^2 E_{brc} \sum_{i=1}^{m} (h_i^2 A_i / \bar{L}_i^3)} = \frac{M_B}{K_B} \tag{12}$$

Note that $\bar{\phi}$ is a function of the overturning moments caused by forces $F_{B,i}$ of Fig. 3a. This implies that the effort to generate a rigid body rotation $\bar{\phi}$ would be resisted by an additional internal overturning moment $M_B$ that tends to restore the structure to its original position. Conversely, the use of supplementary devices such as BRBs would tend to reduce the effects of the external overturning moments $M_0$ by as much as $M_B$. However, if $M_B$ corresponds to $\bar{\phi}$ at first yield, then the total carrying capacity of the system can be estimated as;

$$\sum_{i=1}^{m} F_{B,plastic,i} x_i = M_{B,plastic} = \sum_{i=1}^{m} T_{plastic,i} \frac{\alpha h_i l}{\bar{L}_i} \tag{13}$$

$T_{plastic,i} = \sigma_{yield} A_i$, is the ultimate axial strength of the brace. While there are no flexural interactions between the elements of the imaginary braced frame and the MF, the braced frame tends to oppose the external overturning moment by a notional moment of resistance related to the axial resistance of its members, i.e.,

$$\phi = \frac{M_0 + M_{P\Delta} - M_B}{K_F} = \frac{M_0 + M_{P\Delta} - \phi K_B}{K_F} \quad \text{or} \quad \phi_F = \frac{M_0 + M_{P\Delta}}{[K_B + K_F]} \tag{14}$$

Once again, if $\phi$ exceeds $\phi_{Rqd.}$ or $K_F$ is deemed inadequate then Eq. (14) may be utilized to asses the additional stiffnesses of the supplementary braces to satisfy the issue, thus;

$$K_B = \frac{M_0 + M_{P\Delta} - \phi K_F}{\phi} \tag{15}$$

However, it may be computationally expedient to deal with a single force $F_{B,m} = T_m l / L_m$ as shown in Fig. 3d that causes constant shear along the height of the imaginary

braced frame, rather than the generalised distribution of forces $F_{B,i}$ of Fig. 3a that result in a stepwise variation of shear along the frame. The brace force distribution due to the former strategy can be expressed as; $T_m = F_{B,m}\bar{L}_m/l, \ldots,\ T_i = F_{B,m}\bar{L}_i/l, \ldots,$ and $T_1 = F_{B,m}\bar{L}_1/l$. This allows all brace cross sectional areas $A_i$ to be related to any known value such as $A_m$, i.e., $A_i = (\bar{L}_i/\bar{L}_m)^3(h_m/h_i)$. Since all brace forces are functions of the same variable $\phi$ and that internal forces of all members, are in static equilibrium, then the global moment due to brace resistance can be directly assessed as; $M_B = T_m lH/L_{brc}$.

*Example 4* Preliminary brace selection.

Assuming that the there are no other supplementary devices, except for the diagonal braces of the last bay of Example 1, compute the axial force and the cross sectional areas of one such brace needed to lower the drift ratio to $\phi = 0.003$ radians. Let $\alpha = 1$ and $E = 29{,}000$ ksi.

**Solution** From Example 1, $\phi = 0.0045365$ corresponds to $M_0 = 10{,}000$ kip ft. For, $\phi = 0.003$ the corresponding moment can be reduced to $M_{0,reduced} = 6613$ kip ft. In other words, $M_B = (10{,}000 - 2{,}204{,}342.55 \times 0.003) = 3387$ kip ft. Resorting to uniform shear strategy described above it may be concluded that $A_{3,4,5,6,7,8,9} = A$ and $A_{1,2} = (25/22.361)^3(10/15)A = 0.932A$ . Equation (12) gives;

$$A = \frac{3387 \times 12^4}{0.003 \times 20^2 \times 12^4 \times 29 \times 10^3[(7 \times 10^2/22.361^3) + (2 \times 15^2/25^3)]} = 1.07 \text{ in}^2.$$

Computer analysis gives; $\Delta_{10} = 3.601$ in, which translates to; $\phi = 3.601/1200 = (0.003)$ and $T_9 = \frac{0.003 \times 10 \times 20 \times 1.07 \times 29{,}000}{22.361^2} = 37.24(36.67)$ kips. Next; $M_B = \frac{T_9 lH}{L_9} = \frac{37.24 \times 20 \times 100}{22.361} = 3330(3382)$ kip ft.

### 3.5 RRCs contribution to restoring moments

The RRC is stabilized by means of two vertical parallel post-tensioned tendons as shown in Figs. 1b, h and 2f. The RRC is acted upon by the interactive overturning moments $(M_Q - M_S)$ corresponding to forces $S_i$ and $Q_m$ and the restoring moments $M_M$ and $M_C$. The interactive force $Q_m$ has been introduced to emphasize the fact that the RRC tends to behave as an upright simply supported beam rather than a fixed base cantilever. However, the static equilibrium of the RRC requires that, $M_Q - M_S = M_M + M_C$. Assuming the RRC is sufficiently stiff and strong, then the restoring moment, $M_C$ developed at the pivot level due to rigid body rotation $\phi$, can be expressed as;

$M_C = T_{RRC}d' = K_C\phi$ and $K_C = d'^2 A_{walltendon,}E/H$. Since $M_C$ opposes $M_0$ without coupling with other components of the structure, then its contribution to the global deformations of the system can be expressed as;

$$\phi = \frac{M_0 + M_{P\Delta} - M_C}{K_F} = \frac{M_0 + M_{P\Delta} - \phi K_C}{K_F} \quad \text{or} \quad \phi = \frac{M_0 + M_{P\Delta}}{[K_F + K_C]} \tag{16}$$

*Example 5* Preliminary core tendon selection.

Assuming that the there are no other supplementary devices, except for the rigid core tendons, compute the cable force needed to lower the drift ratio to $\phi = 0.003$ radians. Assume $d' = 10$ ft.

**Solution** From Eq. (16); $M_C = T_{RRC}d' = M_0 - \phi K_F = (10{,}000 - 2{,}204{,}342.55 \times 0.003) = 3387$ kip ft. Therefore, $T_{RRC} = 3387/10 = 338.7$ kips (339.0).

### 3.6 Global response of the RCMF (under $M_0, M_M, M_B$ and $M_C$)

The purpose of this section is to utilize the material presented in the last three sections in order to develop the RCMF characteristic formula. The fully supplemented structure is subjected to external and interactive forces $F_i$ and $(Q_m - S_i)$ respectively, as illustrated in the free body diagrams of Fig. 1c–f. The drift functions (7), (8), (12) and (16) can be utilized to formulate the global drift equation of the subject RCFM, provided that the unknown quantity $(M_Q - M_S)$ can either be determined or assigned a value in terms of $(M_M + M_C)$. Following the rationale leading to Eqs. (10) and (14), it may be concluded that;

$$\begin{aligned} \phi &= \frac{M_0 + M_{P\Delta} + M_Q - M_S - M_B}{K_F} - \frac{M_M}{K'_F} \quad \text{or} \\ \phi &= \frac{M_0 + M_{P\Delta} - (M_B + M_M + M_C)}{K_F} - \frac{M_M}{K'_F} \end{aligned} \tag{17}$$

where $(M_M + M_C)$ has been substituted for $(M_Q - M_S)$. Next, substituting for $M_C = K_C\phi, M_M = K_L\phi$ and $M_B = K_B\phi$ into Eq. (17), it gives after simplification and rearrangement;

$$\phi = \left[\frac{K'_F(M_0 + M_{P\Delta})}{K_F K_L + K'_F(K_F + K_L + K_B + K_C)}\right] = \frac{M_0 + M_{P\Delta}}{K^*} \tag{18}$$

$K^*$, may be interpreted as the global rotational stiffness of the RCMF. It is instructive to note that as the MF becomes a mechanism, i.e., as $K_F$ and $K_M$ tend toward zero, the structure becomes more flexible. It sustains larger but stable lateral displacements due to the resistive nature of the supplementary devices. In other words Eq. (18) reduces to;

$$\phi = \left[\frac{1}{2K_L + K_B + K_C}\right](M_0 + M_{P\Delta}) \tag{19}$$

Equation (19) constitutes a lower bound solution to the failure conditions of the subject RCMF. Denoting $\mathrm{M} = K_F\phi$ as the total moment of resistance of the free standing MF and observing that $(K_F/K_M)$ becomes unity as $k_{i,j}$ approached zero, then the second of Eq. (16) may be rewritten as; $\mathrm{M} = M_0 + M_{P\Delta} - (M_B + 2M_M + M_C)$. This together with Eq. (19) constitute a complete lower bound solution to the failure of the RCMF under consideration.

### 3.7 The global *P*-delta effect

*P*-delta moments adversely influence the performance of all structures during all phases of loading (Hamburger et al. 2009). However, their effects on RCMFs become even more pronounced at incipient collapse. In this section, first the destabilizing effects of the gravity loads on the undamaged MF are studied and expressed in a simple formula, then an attempt is made to estimate the tendon force needed to prevent the catastrophic failure of the RCMF after the frame becomes a mechanism. The *P*-delta moment of any subframe can be expressed as; $P_i\delta_i = \phi h_i \sum_{j=1}^{1} W_{i,j} = \bar{F}_i h_i$, or $\bar{F}_i = \phi \sum_{j=1}^{1} W_{i,j} = P_i\phi$, where $\bar{F}_i$ is the notional equivalent lateral load acting on the subframe. The notional shear force and

rocking moment on any subframe can now be estimated as $V_i = \sum_{r=i}^{m} \bar{F}_r = \phi \sum_{r=i}^{m} P_r$ and $\bar{M}_i = \bar{V}_i h_i$ respectively. If $P_i = P$ then $\bar{F}_i = P\phi = \bar{F}$, $V_i = P\phi(m+1-i)$ and $\bar{M}_i = P\phi(m+1-i)h_i$. The global $P$-delta moment acting on the structure can be computed as the sum of the subframe $P$-delta moment;

$$M_{P\Delta} = P\phi \sum_{i=1}^{m} (m+1-i)h_i = \bar{P}\phi\bar{H} \tag{20}$$

where $\bar{P}$ and $\bar{H}$ may be construed as the sum and of forces $P_i$ and the location of the resultant of story shears $\bar{V}_i$ respectively (the self weight of the wall can be included in $P_i$). It can easily be shown that for $h_i = h$; $\bar{H} = (m+1)mh/2$. Equation (20) may be now be adjusted to include the corresponding $P$-delta or $M_{P\Delta}$ effect, thus; $\phi = (M_0 + \bar{P}\phi\bar{H})/K^*$ or $\phi = M_0/f_{CR}K^*$. $f_{cr} = [1 - (\bar{P}\bar{H}/K^*)]$ is generally defined as the global displacement magnification or load reduction factor.

### 3.8 Determination of interactive forces

If $\theta_{col.F}$, and the contributions of the BRBs and LBs are known, then the magnitude and directions of the interactive forces can be related to total moments acting on any subframe. These forces are needed to design and or upgrade the elements of the RRC in accordance with project requirements. It is expedient to group the external moments $(M_{0,i} + M_{P\Delta,i})$ and device generated moments $\mathrm{M}_{Dev.i} = (M_{M,i} + M_{B,i} + M_{C,i})$ acting on any subframe $i$. The sum of moments of resistances of columns of any subframe, $r$ can be computed as;

$$\mathrm{M}_{col.r} = 2\sum_{j}^{n} M_{col.r,j} = \frac{(M_0 + M_{P\Delta} - M_{Dev.})\sum_{j}^{n} \bar{k}_{r,j}}{\sum_{j=0}^{n}\sum_{i=1}^{m} \bar{k}_{i,j}} \tag{21}$$

The sum of moments of resistances of all columns above level $i$ can be computed as;

$$\bar{\mathrm{M}}_{col.i} = 2\sum_{i=r}^{m}\sum_{j}^{n} M_{col.r,j} = \frac{(M_0 + M_{P\Delta} - M_{Dev.})\sum_{i=r}^{m}\sum_{j}^{n} \bar{k}_{r,j}}{\sum_{j=0}^{n}\sum_{i=1}^{m} \bar{k}_{i,j}} \tag{22}$$

Consider the racking equilibrium of the columns of the uppermost subframe, $i = m$, of Fig. 1d i.e.,

$$(F_m + Q_m - S_m)h_m = \mathrm{M}_{col.m} \quad \text{or} \quad S_m - Q_m = F_m - \frac{\mathrm{M}_{col.m}}{h_m} \tag{23}$$

Similarly, the racking equilibrium of the columns of the subframe at $m-1$ can be expresses as; $(F_m + F_{m-1} + Q_m - S_m - S_{m-1})(h_m + h_{m-1}) = \bar{\mathrm{M}}_{col,m-1}$. Substituting for $(Q_m - S_m)$ from Eq. (23) gives;

$$S_{m-1} = F_{m-1} + \frac{\bar{\mathrm{M}}_{col.m}}{h_m} - \frac{\bar{\mathrm{M}}_{col.m-1}}{(h_m + h_{m-1})} \tag{24}$$

The generalized equilibrium equation of the MF, in terms of the interactive forces at level $i$, can be expressed as;

$$\sum_{r=i}^{m-1}(F_r - S_r)\sum_{s=i}^{r} h_s + (F_m + Q_m - S_m)\sum_{r=i}^{m} h_r = \bar{\mathrm{M}}_{Col,i} \tag{25}$$

Once $(Q_m - S_m)$ and $S_{m-1}$ are known using Eqs. (23) and (24) respectively, $S_{m-2}$,… $S_1$ can be computed through systematic use of Eq. (25) as demonstrated in Example 6 below. The limitations of Eqs. (19) and (25) are discussed in Sect. 3.9 below.

*Example 6* Computation of interactive forces: Compute the interactive forces of Example 1. Assume $M_{P\Delta} = 0$.

**Solution** From Example 1, $M_0 = 10{,}000$ kip ft, $\sum_{j=0}^{n}\sum_{i=1}^{m}\bar{k}_{i,j} = 39{,}294/h$ and $\mathrm{M}_{Dev,i} = 0$. For $i = 1$, and 2: $\sum_{j=0}^{n}\bar{k}_{i,j} = (2\times 448 + 9\times 890)/1.5h = 5937.33/h$, For $i = 3$, 4, 5, 6, 7, 8 and 9:

$$\sum_{j=0}^{n}\bar{k}_{i,j} = (2\times 199 + 9\times 391)/h = 3917/h\ \mathrm{M}_{col,3}, \mathrm{M}_{col,4}, \ldots \mathrm{M}_{col,9} = \frac{M_0\sum_j^n \bar{k}_{m,j}}{\sum_{j=0}^{n}\sum_{i=1}^{m}\bar{k}_{i,j}}$$

$$= \frac{10{,}000\times 3917}{39{,}294} = 996.85 \text{ kip ft}$$

$$\mathrm{M}_{col,1}, \mathrm{M}_{col,2} = \frac{M_0\sum_j^n \bar{k}_{m,j}}{\sum_{j=0}^{n}\sum_{i=1}^{m}\bar{k}_{i,j}} = \frac{10{,}000\times 5937.33}{39{,}293.7} = 1511.02 \text{ kip ft}$$

From Eq. (23); $Q_9 - S_9 = -F_9 + \frac{\bar{\mathrm{M}}_{col,9}}{h_9} = -100 + \frac{996.8512}{10} = -0.315$ kips.

From Eq. (24); $S_8 = 0 + \frac{\bar{\mathrm{M}}_{col,9}}{h_9} - \frac{\bar{\mathrm{M}}_{col,8}}{h_8+h_9} = 0 + \frac{996.8512}{10} - \frac{2\times 996.8512}{20} = 0$. It follows that $S_7 = S_6 = S_5 = S_4 = S_3 = 0$. This indicated that subframes 3 through 9 can be categorized as MFUS. Next, considering the static equilibrium of level 2, Eq. (25) gives; $(100 - 0.31488)(7\times 10 + 15) + S_2\times 15 = (996.85\times 7 + 1511.02)$, or $S_2 = 1.05$ kips

A consideration of static equilibrium at level 1 gives;

$(100 - 0.31488)\times 100 - 1.04954\times 30 - S_1\times 15 = (996.85\times 7 + 1511.02\times 2)$, or $S_1 = 0$. Comparing Examples 1 and 2, it may be seen that the moment frame of Example 2 is not suitable for RCMF applications.

### 3.9 Limitations and applications

The power of Eqs. (18) and (19) lies not only in addressing a multitude of target drift ratios but also in providing a wide range of design strategies, including the two limiting conditions where the use of RCMF combination can be either highly efficient or entirely counterproductive. Two extreme but important cases arise, $S_i = 0$, and $S_i = F_i$. They lead to the development of two distinct classes of structures, MFUR and MFUS respectively. Both cases result in MFs of minimum weight. In the first instant, no interaction takes place between the moment frame and the RRC, i.e., $S_i = 0$, the rigid core and the moment frame tilt compatibly. This can happen, if the core instead of imposing a straight line profile on the frame, adapts the linear displacement profile of the frame under the same lateral loading. In conclusion, it would be counterproductive to use un-supplemented RRCs in conjunction with an MFUR. The second extreme scenario, the MFUS, manifests itself if the core absorbs the entire external loading, i.e. $S_i = F_i$ (assuming the beams are axially rigid). This is the most common condition in practice and happens if the MF is not an

MFUR, is augmented with supplementary devices and/or the core is provided with rotational resistance. Under such circumstances the RRC behaves as an upright simply supported beam with end reactions $Q_m$ and $Q_0$ as shown in Fig. 1. The generic design of an efficient MFUS is presented in Example 9 below.

## 4 Global plastic response of the frame

Seismic response is associated with ultimate loading conditions, and as such maximum carrying capacity of any structure at incipient collapse should be carefully studied (Mazzolani 1997; Goel et al. 2010). Consider the global load carrying capacity of the free standing MF of Fig. 4b under gravity forces $W_{ij}$, $P$-delta moments $M_{P\Delta}$, lateral loading $F_i$, opposing brace moments $M_B$, LB moments $M_M$ and RRC base moments $M_C$.

If the lateral forces are nil or very small then each loaded span will eventually collapse through a beam failure mechanism, as in Fig. 4a, at its maximum carrying capacity;

$$W_{i,j}a_{i,j} = 4M_{i,j}^P L_j/b_{i,j} = 4M_{i,j}^P \delta_{i,j}^P \tag{26}$$

where the Kroneckar's $\delta_{i,j}^P = L_j/(L_j - a_{i,j})$ for $L_j > a_{i,j} \geq 0$ and $\delta_{i,j}^P = 0$ for $a_{i,j} = L_j$. Barring instabilities, the global gravity carrying capacity of the frame can be estimated as $W = \sum_{j=1}^{n} \sum_{i=0}^{m} W_{i,j}$. However, if lateral and gravity loads occur together then two other modes of collapse, depending on the relative magnitudes of the two can also take place. Assuming $W_{i,j}$ is small enough for the frame to fail through a purely sway mode of collapse with plastic hinges forming at beam ends only, as in Fig. 4c, and that the LBs generate a total of $2M_M$ moments at their ends, then the lateral carrying capacity of the system can be estimated as;

$$M_0 + M_{P\Delta} - (M_B + 2M_M + M_C) = \sum_{j=1}^{n} \sum_{i=0}^{m} 2M_{i,j}^P \tag{27}$$

Since Eqs. (2), (12) and (27) coincide, the solution is exact and in conformity with the requirements of the uniqueness theorem (Foulkes 1953). On the other hand, if some of the gravity forces are large enough to cause combined collapse modes in their own spans, such as that shown in Fig. 4b, while all other beams remain straight with plastic hinges at their ends, then the lateral carrying capacity of the system may be re-evaluated as;

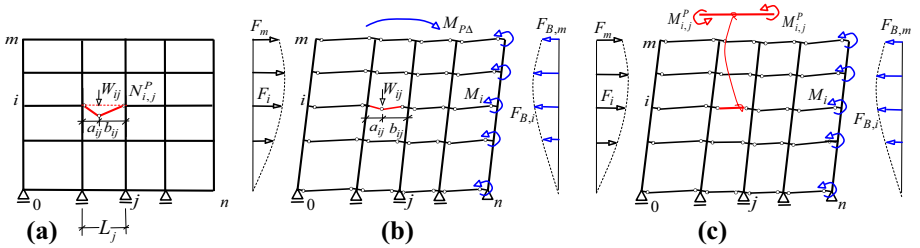


**Fig. 4** **a** Purely beam mechanism, **b** mixed (combined beam + sway) mechanisms, **c** purely sway mechanism

$$\sum_{j=1}^{n}\sum_{i=0}^{m} W_{i,j}a_{i,j} + M_0 + M_{P\Delta} - M_B - 2M_M - M_C = \sum_{j=1}^{n}\sum_{i=0}^{m} 2M_{i,j}^{P}(1+\delta_{i,j}^{P}) \tag{28}$$

A comparison of Eqs. (27) and (28) shows that the two lateral failure modes coincide when;

$$\sum_{j=1}^{n}\sum_{i=0}^{m} W_{i,j}a_{i,j} = \sum_{j=1}^{n}\sum_{i=0}^{m} 2M_{i,j}^{P}\delta_{i,j}^{P} \tag{29}$$

A satisfactory solution is found if matching terms in either side of (29) are made equal, i.e.,

$$W_{i,j}a_{i,j} = 2M_{i,j}^{P}L_j/b_{i,j} = 2M_{i,j}^{P}\delta_{i,j}^{P} \tag{30}$$

Comparing Eqs. (26) and (30) reveals that small floor loads, $W_{Small} \leq 2M^P L/ab$, have no effect on the lateral carrying capacity of the frame. Furthermore, comparing $W_{Small}$ with $W_{Limit}$ and an intermediate $W = 2M^P c/ab$ where $c$ is an arbitrary quantity defined as; $L \geq c \geq a$, it gives;

$$\left[W_{Limit} = \frac{2M^P L}{ab}\right] \geq \left[W = \frac{2M^P c}{ab}\right] \geq \left[W_{Small} = \frac{2M^P a}{ab}\right] \tag{31}$$

Formula (31) can be utilized to assess the plastic limit states of the frame at a glance. It may be seen that in general $W_{Small} \leq (a/L)W_{Limit}$. This gives credence to the notion that; the magnitude of load $W$ at distance "$a$" has little to no effect on the lateral response of the frame if it is less than ($a/L$) of its plastic collapse value acting alone on the same beam. Conversely, if the subject system is designed for increased moments, $(c/a)M^P$, then the lateral carrying capacity of the moment frame will not be affected by the presence of $W$ at "$a$." The ratio (c/a) may be referred to as the moment adjustment factor for the beam $ij$. Under such conditions the beams may be said to have attained the effective strength needed to support the full development of the frame response at ultimate loading. However it should be kept in mind that any increase in the carrying capacity of the structure also increases the magnitude of the corresponding $P$-delta effects. An elaboration of the small load concept can be found in Grigorian and Grigorian (2012).

*Example 7* Demonstration of small load concept.

The MF of Example 1 is subjected to simultaneous applications of a lateral force $F = 100$ kips at roof level and a central concentrated loads $W = 5M^P/2$ on each beam, except at roof and grade levels where $W_{0,j} = W_{m,j} = W/2$. The plastic strengths of the roof and grade level beams are given as $M^P/2$. The plastic strength of all other beams is $M^P$.

Compute the minimum strength of the MF such that it fails through a purely sway mode of collapse.

**Solution** $a = b = L/2$. Formula (31) can be used to compare the plastic failures modes of the frame as;

$$(W_{Limit} = 8M^P/L) \geq (W = 5M^P/L) \geq (W_{small} = 4M^P/L),$$

with the obvious conclusion that the strength of the beams should be adjusted by a factor of ($c/a = 5/4$).

*Example 8* *P*-delta effects at incipient collapse.

Following Example 6, compute the magnitude of $M_{P\Delta}$ due to increased beam strengths, $W = 5M^P/L$.

**Solution** The lateral carrying capacity of the frame in the absence of the *P*-delta moments can be computed from $Fmh = 2nmM^P$, i.e. $F = 2nM^P/h$. The virtual work Eq. (30) gives; $\phi M_{P\Delta} = n\frac{W}{2}m\phi h + nW\sum_{i=1}^{m-1} i\phi h = nm(m+1)\phi hW/2 = 5nm(m+1)\phi hM^P/2L$ and Eq. (20) leads to; $F = \frac{2nM^P}{h}\left[1 - \frac{5(m+1)h\phi}{4L}\right]$. In other words, if the subject structure is to perform as expected at ultimate loading then the prescribed drift ratio should be much smaller than; $\phi < [4Ll/5(m+1)h]$.

## 5 Collapse prevention and self centering

The fundamental assumption adapted in this section is that the MF and some of the supplementary devices can act as hysteretic elements and that at least one group of elements are capable of preventing catastrophic collapse. The applications of the proposed concepts to collapse prevention and self centering are best illustrated through the forthcoming parametric example. Permanent deformations and structural collapse are foreseeable phenomena associated with diminishing and exhausted energy absorption capacities respectively. Collapse prevention, in this context, refers to the ability to provide temporary support for the gravity system, after a major seismic event until a repair or demolition program is implemented. It also means that there is at least one reliable source of energy absorption that can sustain additional deformations until the seismic event is completely over. Here, self-centering is defined as the ability that tends to realign a structural mechanism back to its original undisturbed form. The purpose therefore is not to prevent the formation of plastic hinges that lead to a failure mechanism, but rather to prevent catastrophic collapse due to *P*-delta and similar effects. However, it should be born in mind that residual deformations under seismic loading can significantly affect the re-centering capacity of the structure (MacRae and Kawashima 1997; Dazio 2004). However, if complete collapse is to be prevented after formation of a preferred plastic mechanism, then the surviving LBs and the vertical cable system should be strong enough to withstand the entire conditional demand. At incipient failure all moment resisting elements except the RRC tendons (or any one group of supplementary devices) become incapacitated. i.e.$K_F = K_M = K_L = K_B = 0$. Subsequently, the global stiffness of the RCMF reduces to $K^* = K_C$. In other words, if building collapse is to be prevented after the formation of the failure mechanism then the core tendons should be strong enough to withstand the entire seismic demand imposed on the system. With $M_0$, $M_{P\Delta}$ and prescribed $\phi$ known, the basic design parameters for collapse prevention can be computed as;

$$T > \frac{\Omega(M_0 + M_{P\Delta})}{d'} = \frac{\Omega\phi K^*}{d'} \tag{32}$$

where $\Omega$ is the over strength factor defined by the pertinent code of practice, $d'$ is the tendon lever arm. See Fig. 1a.

### 5.1 The rules of sequential failures

According to rules of sequential failures if the deformations of a member comparable structures connected in parallel, such as RCMF of Fig. 1a, can be related to the same single variable then the three basic rules of plastic failures can be stated as follows.

1. Order of sequential failure is the same as the ascending order of plastic displacements of each system.
2. Maximum deformation of the combined system at first yield is the same as that of the first failing structure.
3. Maximum deformation of the combined system at incipient collapse is that of the last failing component.

This implies that if $(M_F^P/K_F) > (M_L/K_L) > (M_B/K_B) > (M_C/K_C)$ then the moment frame will fail first followed by sequential failures of the LBs, BRBs and the RRC.

## 6 Applications and limitations of RCMFs

The proposed structural system lends itself well to performance control through the use of different types of supplementary devices. Equation (17) covers a wide spectrum of modes of response for all loading conditions. However, it provides no information regarding the suitability, efficiency and limitations of RCMFs as earthquake resisting systems. A practical way of evaluating the usefulness of such systems is to study the nature of the interactive forces $Q_m$ and $S_i$ with a view to the functional requirements of the main components of the structure. The effects of the supplementary devices on the RRC and the MF have been amply described in the preceding sections.

### 6.1 Limitations

The focus of the current section is on the interaction of the RRC and the MF in the absence of auxiliary devices. Two extreme scenarios come to mind. First, no interaction takes place between the MF and the RRC. i.e., $S_i = Q_m = 0$, while the rigid core and the moment frame tilt compatibly. This can happen, if instead of imposing a straight line profile on the frame, the core adapts the linear displacement profile of the frame under the same lateral loading. In conclusion, it would be counterproductive to use un-supplemented RRCs in conjunction with a MFUR. Comparing Examples 1 and 2, it may be seen that the MF of Example 2 is not suitable for RCMF applications.

### 6.2 Applications

The second extreme scenario manifests itself if the beams are axially rigid and the core absorbs the entire external loading, i.e. $S_i = F_i$. This is the most commonly occurring condition in practice and happens if the MF is not an MFUR, is augmented with supplementary devices and/or the core is provided with rotational resistance. Under such circumstances the RRC behaves as an upright simply supported beam with end reactions $Q_m$ and $Q_0$ as shown in Fig. 1h. The complete parametric solution of a typical MFUS is provided in Example 9 below. The materialization of a generic MFUS, in the form of a new earthquake resisting building with self centering and collapse prevention capabilities is presented in Sect. 7 of the current article.

*Example 9* Structural design of an efficient un-supplemented RCMF.

Design an efficient, $m \times n$ regular RCMF, under a triangular distribution of lateral forces; $F_i = Fi/m$, and axial nodal forces $P_i = P$ to sustain a uniform drift ratios $\phi_Y$ and $\phi_P$ at first yield and incipient collapse respectively. Let; $h_i = h$, $L_j = L = 2h$,$J_{i,0} = J_{i,n} = J$ all other $J_{i,j} = 2J$, $I_{0,j} = I_{m,j} = I$, all other $I_{i,j} = 2I$. Assume $I = J$.

**Solution** For initial member sizing it is prudent to assume that the system is totally un-supplemented, i.e., $M_B = M_M = M_C = 0$. $V_i = Q$ and $V_i h_i = Qh$ are constant. Equation (7) gives; $\frac{1}{K^*} = \frac{1}{K_F} = \frac{1}{24mnE}\left[\frac{h}{J} + \frac{L}{I}\right] = \frac{h}{8mnEI}$. Since MFUS are associated with $S_i = F_i$, then according to Fig. 1c, g the entire seismic load would be transmitted to the rigid core. The static equilibrium of the rigid core requires that; $Q_m H = M_0 + M_{P\Delta} = \phi K^*$ or, $\frac{m(m+1)[(2m+1)F+3P\phi]h}{6} = \phi K^*$. Consequently; $I_{i,j} = J_{i,j} = \frac{(m+1)[(2m+1)F+3P\phi]h^2}{48nE\phi}$. Similarly the static equilibrium of any row of columns give $4nM_{col.i,j} = Qh$ or $M_{col.i,j} = \frac{m(m+1)[(2m+1)F+3P\phi]h}{24n}$. Except for $M_{col.i,0} = M_{col.i,n} = M_{col.i,j}/2$. It follows that the plastic moment of resistance of the MF based on a beams only failure mechanism can be computed as; $M^P_{0,j} = M^P_{m,j} = M^p$ and all other $M^P_{i,j} = 2M^P$.

The static equilibrium of the MF at incipient collapse, due to $F_P$ gives $Q_m H = M_0 + M_{P\Delta} = 4mnM^P$ or, $M^P = \frac{m(m+1)[(2m+1)F_P+3P\phi_P]h}{24n}$. This completes the preliminary member sizing of the moment frame.

### 6.3 Structural design of the RRC

Whatever the material or the configuration of the RRC, a steel braced frame, reinforced concrete or steel plate shear wall, it should be sufficiently strong and rigid in order to perform its functions as part of the lateral load resisting system, i.e., to withstand the external forces, prevent soft story failure in the MF and provide support for the supplementary devices. As a precautionary measure it would be safe to assume that the RRC alone is capable of withstanding the ultimate earthquake induced and *P*-delta effects. Since the RRC acts as an upright simply supported beam or truss girder, the corresponding distribution of bending moments due to $F_{P,i} = F_P i/m$ and $\bar{F}_i = P\phi = \bar{F}$ at any elevation $i$ can be expressed as;

$$M_{core,i} = \frac{F_P ih}{6m}\left[(m^2 - 1) - (i^2 - 1)\right] + \frac{\bar{F}ih}{2}[(m - 1) - (i - 1)] \tag{33}$$

If the flexural design of the core is based on Eq. (33) then it could easily prevent soft story failure of the MF.

### 6.4 Determination of wall stiffness

Ideally speaking the core should be infinitely rigid. However if the rigidity of the RRC, $E_w I_w$, were to be large but finite, its magnitude could be related to its maximum end rotation $\psi_w$, Fig. 2g, or its maximum drift ratio. With $\psi_w$ at hand, the stiffness of the wall can be related to a fraction of the prescribed uniform drift $\phi$ of the system, say $5\%\phi$. If this is true then a workable design value for the moment of inertia of the wall can be estimated as $\psi_{\max} = \varepsilon\phi$. The maximum slope of the core due to $F_{P,i} = F_P i/m$ and $\bar{F}_i = P\phi = \bar{F}$ can be expressed as;

$$\psi_{\max} = \frac{F_P h^2 (m-1)(2m-1)(2m^2+3m-4)}{180 E_w I_w m} + \frac{\bar{F} h^2 m (m-1)(m^2+m-2)}{24 E_w I_w} \tag{34}$$

$$I_{w,\min} = \frac{F_P h^2 (m-1)(2m-1)(2m^2+3m-4)}{180 E_w \varepsilon \phi m} + \frac{\bar{F} h^2 (m-1)(m^2+m-2)}{24 E_w \varepsilon \phi} \tag{35}$$

## 7 The proposed building system

The generic plans of the proposed new building system incorporating RCMF technologies are presented in Figs. 5 and 6. In this scheme the essential earthquake resisting systems are placed along the perimeter and the central line of the long side. The blue sections mark the link beams. All columns are grade beam supported. As a design option the interior non-RCMFs may be detailed as simple MFs only. The subject earthquake resisting system consists of four essential components; The GBSMF, the RRC, the LBs and the stabilizing tendons. The system is capable of accommodating BRBs and similar supplementary devices.

- The gravity system and the earthquake resisting MF are designed in accordance with the rules and regulations of the prevailing codes of practice with provisions to accommodate the unbonded stressed tendons and special attention to the week beam–strong column requirement. The additional moments induced by the LBs should be taken into account when designing the column affected by gap opening.
- The RRC should be free to pivot about its base and rotate freely at all slab wall junctions. Figure 8 show one such detail that allows horizontal shear transfer from the slab to core without inhibiting the vertical component of the rocking movement at the same junction. The detail also provides out of plane stability at all floor levels.

The most commonly utilized post-tensioned gap opening LB system with butting flat ends against column sides tends to expand the frame beyond its original span length (Sause et al. 2006). As the gap widens at the beam–column interface, the LB rotates upwards, and bends the column inwards (Chou and Chen 2008). This in turn opposes the post-tensioning force. Note that in this particular case the angle of rotation of the column, $\psi$ is larger than $\phi$. In order to alleviate or reduce these effects, the senior author has proposed the use of a

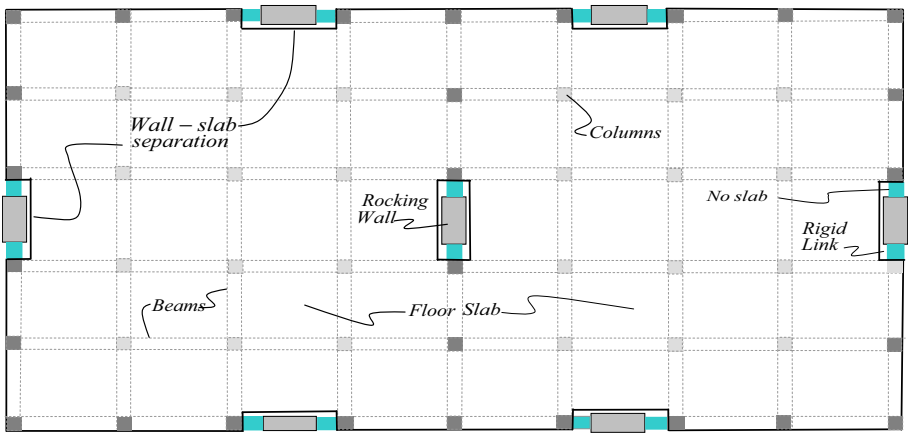


**Fig. 5** Generic floor plan showing physical separation between RRC, LB and diaphragm

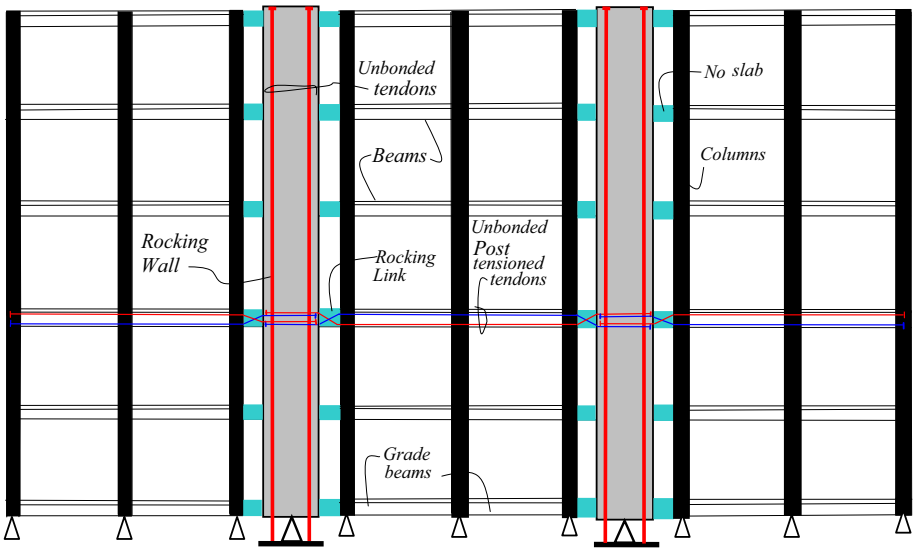


**Fig. 6** Generic RCMF with post-tensioned LBs and RRC

truncated version of the same LB as shown in Fig. 7a, c. The proposed LB consists of a coaxial rigid compression elements surrounded by a reinforced concrete cage that holds the PT tendons together and provides stability for the axial core. It follows that in order to prevent contact between the column and the truncated end of the LB the width of the initial gap should be larger than $\bar{\phi}d/2$. Instead of using axial springs at the ends of the LBs and the wall base, equivalent rotational schemes have been utilized to capture the restraining effects of the post tensioned tendons. See Appendices 1 and 2 below.

- Post-tensioning cables and their attachments are commercially available. Their disposition along the length of the frame, the LBs and the RRC should be in strict conformance with the pertinent engineering principles. While it is good practice to extend the tendons from end to end as shown in Fig. 6, their length, layout cross

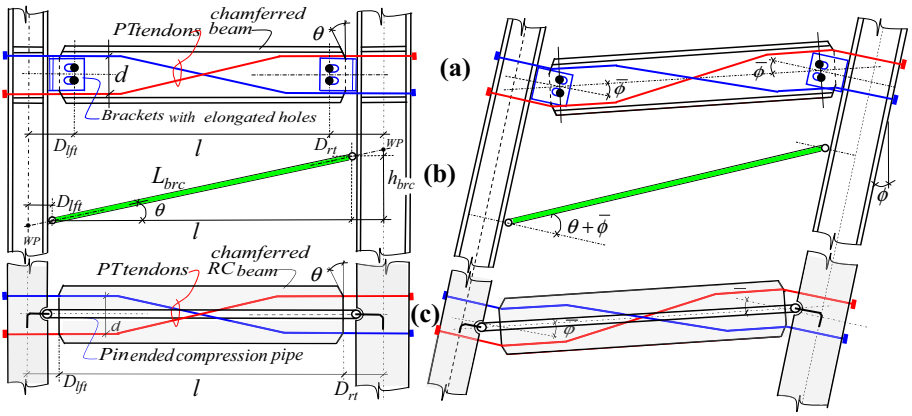


**Fig. 7** (*a*) Chamfered steel LB before and after rotation, (*b*) BRB before and after rotation, (*c*) chamfered reinforced concrete LB before and after rotation

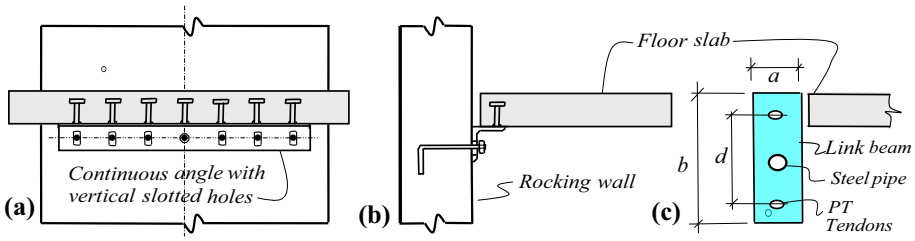


**Fig. 8** **a** Symbolic wall-slab shear connection, **b** section showing same, **c** link beam section

sectional areas and the pre-stressing forces should be assessed in terms of the required drift angle, self centering and collapse prevention requirements (Kurama et al. 1998; MacRae and Priestley 1994).

- The slab acts as a rigid horizontal diaphragm. Seismic shear is transferred to the RCMF system through stressed tendons, compression of the LB, as well as direct shear connectors between the slab and the wall, Fig. 8. The physical separation between the slab and the wall and the LB, Fig. 8 prevents the slab from being damaged during strong ground motion.

## 8 Conclusions

A new earthquake resisting structural system incorporating post tensioned RRCs and MFs has been presented. Vertical and horizontal stressed tendons, gap opening devices as well as BRBs have been provided to ensure collapse prevention and active re-centering. Both Horizontal and vertical post-tensioned devices produce resisting moments to service loading along the frame and provide restoring forces that tend to return the damaged MF and the RRC to their pre-earthquake position. The paper also provides a basis for developing sustainable earthquake resisting structures in the future.

Global Design Led analysis which is a new analytic approach has been used to develop exact, closed form solutions for RCMFs under gravity and lateral loading conditions. The proposed mathematical model is ideally suited for manual preliminary design of such systems. The proposed configuration is both construction friendly and satisfies the theoretical conditions of minimum weight design. Several examples have been provided to verify and demonstrate the applications of the proposed formulations. Two new gap opening link mechanisms, one for steel and the other for concrete structures that do not induce unwanted moments in the columns have also been introduced.

The success of the proposed formulations, as compared with classical methods, lies in the provision of the necessary means that lead to the prescribed objectives rather than investigating the validity of randomly developed initial schemes. For instance, the adaption of grade beam-supported, pinned base columns, as opposed to fixed boundaries, allow the entire structure to respond as a truly controllable rocking systems. However, the proposed structural scheme is neither perfect nor complete. It is still under development and needs the test of time and scrutiny before it becomes a viable earthquake resisting system.

**Acknowledgements** The present paper was written during senior author's tenure at the International Institute of Earthquake engineering and Seismology, IIEES, Tehran, Iran. The hospitality and cooperation of the management of the IIEES is duly acknowledged.

## Appendix 1: Gap opening angle

The analysis relating the gap opening angle to the drift ratio can be summarizes as follows. Let all columns rotate $\phi$ as shown in Fig. 7a, c. Let $\Delta_{left} = \phi D_{lft}$ and $\Delta_{lrightt} = \phi D_{rt}$ represent the fall and rise of the ends of the link beam respectively. The total rotation of the gap and or the brace of Fig. 7b can be formulated as;

$$\bar{\phi} = \phi + (\Delta_{left} + \Delta_{right})/l = (l + D_{lft} + D_{rt})\phi/l = \alpha\phi. \tag{36}$$

## Appendix 2: Change in length of a diagonal brace

The axial displacements of any diagonal brace such as that shown in Fig. 7b can be related to the common drift ratio $\phi$ as follows. The original length of the brace can be computed as $L_{brc}^2 = l^2 + h_{brc}^2$. If $\Delta_h = \bar{\phi} l$ is the change in heights of the two ends of the brace then the new length can be estimated as $\bar{L}_{brc}^2 = l^2 + (h_{brc} + \Delta_h)^2$. After omitting the small quantity $\Delta_h^2$, the change in length can be computed as;

$$\Delta_{brc} = (\bar{L}_{brc} - L_{brc}) = \frac{\Delta_h h_{brc}}{L_{brc}} = \frac{\alpha\phi h_{brc} l}{L_{brc}} \tag{37}$$

## References


Ajrab J (2000) Rocking-wall frame structures with supplemental damping devices. MS thesis, State University of New York at Buffalo, Buffalo, NY

Ajrab J, Pekcan G, Mander J (2004) Rocking wall–frame structures with supplemental tendon systems. J Struct Eng 130(6):895–903

ASCE (2007) Seismic rehabilitation of existing buildings. ASCE/SEI Standard 41-06 with supplement 1. American Society of Civil Engineers, Reston

Aslam M, Goddon WG, Scalise DT (1980) Earthquake rocking response of rigid bodies. J Struct Div ASCE 106(2):377–392

Brandt A (1978) Criteria and methods of structural optimization. Kluwer Academic Publications, Dordrecht

Chancellor NB, Eatherton MR, Roke DA, Akbas T (2014) Self-centering seismic force resisting systems: high performance structures for the city of tomorrow. Buildings 4:520–548

Chou CC, Chen JH (2008) Column restraining effects in post-tensioned self-centering moment frames. In: The 14 world conference on earthquake engineering, Beijing, China, 12–17 October 2008

Dazio A (2004) Residual displacements in capacity designed reinforced concrete structures. In: The 13th world conference on earthquake engineering, Vancouver, BC, Canada

Deierlein GG, Ma X, Eatherton M et al (2009) Collaborative research on development of innovative steel braced frame systems with controlled rocking and replaceable fuses. In: Proceedings of 6th international conference on urban earthquake engineering, Tokyo, pp 413–416

Deierlien GG, Reinhorn AM, Willford MR (2010) Non-linear structural analysis for seismic design. NEHRP Seismic Design Technical Brief No. 4, Gaithersburg, MD, NIST GCR 10-917-5

Dowden DM, Bruneau M (2011) New Z-BREAKSS: post-tensioned rocking connection detail free of beam growth. AISC Eng J 48(2):153–158

FEMA (2005) Improvement of nonlinear static seismic analysis procedures. FEMA report 440, Washington, DC

FEMA (2009) NEHRP recommended seismic provisions for new buildings and other structures. FEMA P-750, Federal Emergency Management Agency, Washington

Foulkes J (1953) Minimum weight design and the theory of plastic collapse. Q Appl Math 10:347–358

Garlock M, Sause R, Ricles JM (2007) Behavior and design of post-tensioned steel frame systems. J Struct Eng ASCE 133(3):389–399

Goel SC, Liao WC, Bayat MR, Chao SH (2010) Performance-based plastic design method for earthquake resistant structures. Struct Des Tall Spec Build 19:115–137
Grigorian M (2015) New directions in earthquake resisting structures. In: 6th International conference on earthquakes and structures, ACECR of Kerman, Iran, pp 301–312
Grigorian M, Grigorian C (2012) Performance control: a new elastic–plastic design procedure for earthquake resisting moment frames. J Struct Div ASCE 138(6):473–483
Grigorian C, Grigorian M (2013) Drift control for multistory moment-frames under lateral loading. Int J High Rise Build 2(4):1–11
Grigorian C, Grigorian M (2015a) Performance control and efficient design of rocking-wall moment-frames. J Struct Div ASCE. doi:10.1061/(ASCE)ST.1943-541X.0001411
Grigorian M, Grigorian C (2015b) An introduction to the structural design of rocking wall-frames with a view to collapse prevention, self-alignment and repairability. Struct Des Tall Spec Build. doi:10.1002/tal.1230
Grigorian C, Popov E, Yang T (1995) Developments in seismic structural analysis and design. Eng Struct 17(3):187–197
Grigorian M, Moghadam SA, Mohammadi H (2017) On rocking core-moment frame design. In: 16th World conference on earthquake engineering, Santiago, Chile, ID#397, 9 January 2017
Hajjar JF, Sesen AH, Jampole E, Wetherbee A (2013) A synopsis of sustainable structural systems with rocking, self-centering, and articulated energy-dissipating fuses. Department of Civil and Environmental Engineering Reports, Report No. NEU-CEE-2013-01, Northeastern University, Boston, Massachusetts, US
Hamburger RO, Krawinkler H, Malley JO, Adan SM (2009) Seismic design of steel special moment frames: a guide for practicing engineers. NEHRP Seismic Design Technical Brief, No. 2, US
Housner GW (1963) The behavior of inverted pendulum structures during earthquakes. Bull Seismol Soc Am 53(2):403–417
Janhunen B, Tipping S, Wolfe J, Mar D (2012) Seismic retrofit of a 1960s steel moment-frame high-rise using a pivoting spine. In: Proceedings of the 2012 annual meeting of the Los Angeles tall buildings structural design council
Ji XD, Kato M, Wang T, Hitaka T, Nakashima M (2009) Effect of gravity columns on mitigation of drift concentration for braced frame. J Constr Steel Res 65(12):2136–2148
Kurama Y, Sause R, Pessiki S, Lu LW, El-Sheikh M (1998) Seismic design and response evaluation of unbonded post-tensioned precast Concrete walls. Precast Seismic Structural Systems Rep. No. 03 (Lehigh Univ., Lehigh, Pa., Rep. No, EQ-97-01)
MacRae GA, Kawashima K (1997) Post-earthquake residual displacements of bilinear oscillators. Earthq Eng Struct Dyn 26(7):701–716
MacRae GA, Priestley MJN (1994) Precast post-tensioned un-grouted concrete beam–column sub-assemblage tests. Report No. SSRP 94/10, Department of Applied Mechanics and Engineering Sciences, University of California San Diego, CA
MacRae GA, Kimura Y, Roeder C (2004) Effect of column stiffness on braced frame seismic behavior. J Struct Div ASCE 130(3):381–391
Mazzolani M (1997) Plastic design of seismic resistant steel frames. Earthq Eng Struct Dyn 26(2):167–169
Miller DJ, Fahnestock LA, Eatherton MR (2011) Development and experimental validation of a nickel–titanium shape memory alloy self-centering buckling-restrained brace. Eng Struct 40:288–298
Panian L, Steyer M, Tipping S (2007) An innovative approach to earthquake safety and concrete construction. J Post Tens Inst 5(1):7–16
Priestley MJN, Tao J (1993) Seismic response of precast prestressed concrete frames with partially debonded tendons. PCI J Precast Prestress Concr Inst 38–1:58–69
Sause R, Ricles J, Liu J, Garlock M, Van Marcke E (2006) Overview of self-centering EQ resistant steel frames research. In: Proceedings of 2nd U.S.-Taiwan workshop on self-centering structural systems, Taipei, Taiwan
Seymour D, Laflamme S (2011) Quasi-static analysis of rocking wall systems. Department of Civil and Environmental Engineering, Massachusetts Institute of Technology, Cambridge
Takeuchi T, Chen X, Matsui R (2015) Seismic performance of controlled spine frames with energy-dissipating members. J Constr Steel Res 114:51–65
Taylor Devices. www.taylordevices.com
Wada A, Qu Z, Ito H, Motoyui S, Sakata H, Kasai K (2009) Seismic retrofit using rocking walls and steel dampers. In: ATC/SEI conference on improving the seismic performance of existing buildings and other structures
Wada A, Qu Z, Ito H, Motoyui S, Sakata H, Kasai K (2012) Pin supported walls for enhancing the seismic behavior of building structures. Earthq Eng Struct Dyn 41:2075–2092